Capacitive Energy Storage on Fe/Li3PO4 Grain Boundaries

ARTICLE *in* THE JOURNAL OF PHYSICAL CHEMISTRY C · FEBRUARY 2011

Impact Factor: 4.77 · DOI: 10.1021/jp111015j

6 AUTHORS, INCLUDING:

Xianwei Guo
Tohoku University
21 PUBLICATIONS **626** CITATIONS
SEE PROFILE

Zhaoxiang Wang
Chinese Academy of Sciences
166 PUBLICATIONS **5,462** CITATIONS
SEE PROFILE

THE JOURNAL OF PHYSICAL CHEMISTRY C

ARTICLE

pubs.acs.org/JPCC

Capacitive Energy Storage on Fe/Li_3PO_4 Grain Boundaries

Xianwei Guo,[†] Xiangpeng Fang,[†] Ya Mao,[†] Zhaoxiang Wang,[*,†] Feng Wu,[‡] and Liquan Chen[*,†,§]

[†]Laboratory for Solid State Ionics, Institute of Physics, Chinese Academy of Sciences, Beijing 100190, People's Republic of China

[‡]School of Chemical Engineering and Environment, Beijing Institute of Technology, Beijing 100081, People's Republic of China

[§]School of Materials Science and Engineering, Chonnam National University, Gwangju, 500-757, Republic of Korea

ABSTRACT: Energy storage was realized on the interfaces between Fe and Li_3PO_4 nanograins in situ fabricated by discharging commercial $LiFePO_4$ to 0.005 V vs Li^+/Li. X-ray diffraction and high-resolution transmission electron microscopy indicate that both the metallic Fe and Li_3PO_4 nanocrystallites are stable up to 4.2 V. The solid electrolyte interphase layer on the nanocomposite does not decompose until 1.7 V according to infrared spectroscopic analysis. The Fe/Li_3PO_4 nanocomposite stores up to 220 mAh g^{-1} of lithium without any electrochemical reactions. This is a purely lithium storage behavior distinct from that on the electrodes of supercapacitors or traditional secondary batteries.

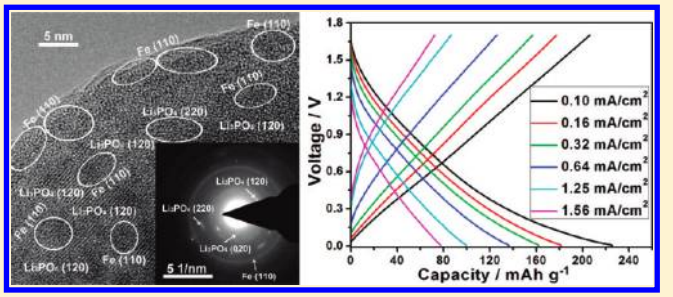

INTRODUCTION

Energy can be electrochemically stored either by reversible adsorption and desorption of the anions and cations on the electrode surfaces of supercapacitors[1] or by insertion and extraction of the ions in/from the lattices of the electrode materials of secondary batteries.[2,3] For both cases, the electrode material can be either a single phase or a composite. Recently, Maier et al.[4] reported another way of energy storage, lithium storage on the interfaces of two distinct phases. They calculated and found it thermodynamically beneficial for the lithium ions and the electrons to be stored on the interior surfaces of two phases, respectively.[5,6] This energy-storage behavior is quite similar to that of the supercapacitors except that the cations and the anions are adsorbed on the exterior surfaces of the electrodes (the particles on the electrodes) of the supercapacitors. Such interfacial lithium-storage behavior has been observed in, but restricted to, conductive/insulating composite thin films, such as Cu/LiF,[6] Ti/Li_2O,[5] Ti/LiF,[7] and Fe/LiF.[8] Balaya et al.[9] reported reversible homogeneous and heterogeneous lithium storage in RuO_2 (or Ru/Li_2O nanocomposite) powder. However, we do not think that RuO_2 can be regarded as a good example for purely interfacial lithium-storage in powder samples because homogeneous (lithium storage by insertion to and extraction from the lattice of RuO_2 single phase) and heterogeneous (Ru/Li_2O interfacial lithium storage) lithium storage coexist in the RuO_2 powder. It is difficult to distinguish these two lithium storage mechanisms even below 1.0 V vs Li^+/Li (please see the shape of the potential profiles in ref 9), as Li_2O can be decomposed and RuO_2 is reformed at low charge potentials due to the catalysis effect of the metallic Ru nanoparticles. Therefore, no purely capacitive behavior has actually been reported on powder electrodes.

Electrochemical conversion reaction is a well-known lithium storage mechanism, especially for the oxides,[10] sulfides,[10] and fluorides[11] of transition metals. The majority of the reversible capacity of these materials comes from the long potential plateau for conversion reaction, $MX + Li^+ + e^- \leftrightarrow LiX + M$ (M is for transition metals and X is for O, S, F, etc.). No reversible capacity will be available if the LiX cannot be decomposed during recharge. This plateau is usually followed by a long slope extending to 0.0 V vs Li^+/Li. Tarascon and coauthors[12,13] attributed this slope to the decomposition of the solid electrolyte interphase (SEI) layers resulting from irreversible electrolyte decomposition. Maier et al.[4] assigned it to lithium storage on the interfaces between LiX and M particles.

Clearly, the capacitive energy-storage behavior is highly dependent on the specific surface areas (SSAs) of the electrode. With modern techniques (pulsed laser deposition/magnetron sputtering, PLD/MS, for example), it is easy to prepare (multilayered) composite thin films with high SSAs. Nevertheless, the SSAs of the powder prepared by traditional methods are usually below 100 $m^2 g^{-1}$. In addition, the nanoparticles tend to aggregate and the SSAs of the powder decrease quickly. Therefore, it is difficult to observe lithium storage on the interfaces of powder composites. However, the above electrochemical conversion reaction provides an effective way to in situ fabricate nanocomposite with very high SSAs. M and LiX nanocrystallites are formed at the end of initial discharge, no matter the size of the original MX particle.

In this work, we report charge/energy storage on the grain boundaries of Fe/Li_3PO_4 nanocomposite by discharging commercial $LiFePO_4$ to 0.005 V vs Li^+/Li. It will be seen that such a nanocomposite can store up to 220 mAh g^{-1} of lithium without any electrochemical reactions.

Received: November 18, 2010
Revised: January 8, 2011
Published: February 14, 2011

EXPERIMENTAL SECTION

Material Preparation. Phase-pure $LiFePO_4$ was purchased in Tianjin STL Energy Technology Co., Ltd. (China). The sizes of the primary particles are 0.5−1 μm. A mixture of Li_3PO_4 and carbon black (9:1 by weight) was high-energy ball-milled on SPEX 8000D (America SPEX CertiPrep Inc.) for 10 h in ethanol in an airtight mortar in order to find out the contribution of carbon black to the observed capacity of the Fe/Li_3PO_4 composite.

Electrochemical Measurement. An *N*-methylpyrrolidone slurry containing 80 wt % $LiFePO_4$ powder, 10 wt % carbon black (CB) and 10 wt % polyvinylidene fluoride as the binder was cast on a titanium (Ti) foil as the working electrode. The electrode containing 5 wt % CB and 85 wt % $LiFePO_4$ was also prepared for reference. Button-type test cells were assembled in an argon-filled glovebox with 1 mol L^{-1} solution of $LiPF_6$ in ethylene carbonate/dimethyl carbonate (EC:DMC = 1:1 v/v) as the electrolyte, fresh lithium foil as the counter electrode and Celgard 2300 as the separator. A typical electrode contained ~2 mg $LiFePO_4$ on an 8 × 8 mm electrode sheet. Fe/Li_3PO_4 nanocomposite was formed (see Results and Discussion) by galvanostatically discharging the $LiFePO_4$/Li cell to 0.005 V vs Li^+/Li. Without being dissembled, the cell was then galvanostatically cycled between 0.005 and 1.7 V (for determining the lithium storage capacity) or higher cutoff charge voltages (for electrochemically processing the material). The current density was set to 0.10 mA cm^{-2} during cycling unless otherwise specified. The electrochemical performances of the Fe/Li_3PO_4 nanocomposite were characterized on Land BT2000 battery tester (Wuhan, P. R. China) at room temperature. Cyclic voltammetry (CV) tests were carried on CHI600D Electrochemical Workstation (Shanghai, P. R. China) at different scan rates between 0.000 and 1.7 V.

To ensure complete oxidation the electrode material for ex situ X-ray diffraction (XRD) and high resolution transmission electron microscopic (HRTEM) analysis as well as Fourier transformed infrared (FTIR) spectroscopic tests, the test cells after several cycles were first galvanostatically charged to the required potentials and then potentiostatically charged at that potential until the current decays to 5 μA or lower. For the discharged cells, the cell was galvanostatically discharged to the required potential, kept there for 10 h and then continue the discharge to the preset potential until the discharge time decays to less than 10 s.

Physical Characterization. The electrode materials were scraped off of the Ti current collector of the cycled cells and rinsed with DMC carefully before being characterized by XRD (Holland X'Pert Pro MPD X-ray diffractometer equipped with a monochromatized Cu−Kα radiation) and TEM (Tecnai G2 F20 U-TWIN). The FTIR spectra of the commercial Li_3PO_4, $LiFePO_4$ and Fe/Li_3PO_4 discharged or recharged to various potentials were collected on EQUINOX55 (Bruker Optics, Germany).

RESULTS AND DISCUSSION

The XRD analysis (Figure 1) indicates that Fe and Li_3PO_4 are the only discharge products of $LiFePO_4$ first discharged to 0.005 V. No $LiFePO_4$ or $FePO_4$ is detected until the electrode is recharged to 4.2 V, indicating that Li_3PO_4 is stable until 4.2 V (Figure 1). The HRTEM images and the selected area electron diffraction (SAED) patterns (insets) of the electrode at different charge/discharge states are shown in Figure 2. Clusters of well-defined stripes are found dispersed in the view field of the electrode material recharged to 4.2 V after having been discharged to 0.005 V. This is clearly due to the $LiFePO_4$ particle pulverization upon repeated lithium insertion and extraction. A close examination to the *d*-spacings calculated from the HRTEM image and the SAED patterns shows that the commercial microsized $LiFePO_4$ particles become clusters or nanograins of Fe and Li_3PO_4 (~5 nm in size). This is supported with the diffused diffraction rings and bright spots in the SAED. The interplanar spacings (*d*-values) of these two species by HRTEM and SAED and JCPDS data of $LiFePO_4$, Li_3PO_4 and metallic Fe are listed in Table 1 for comparison. The Fe and Li_3PO_4 grains (2−3 nm in size) are randomly dispersed in the sample. No other species were detected. The interfaces between Fe and Li_3PO_4 crystallites are not clear.

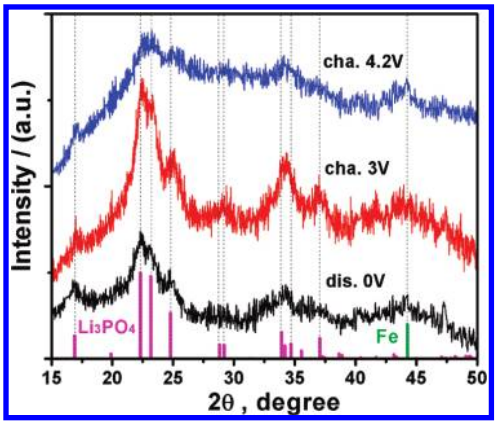

Figure 1. Recognition and structural stability of the discharge products of $LiFePO_4$ at various charge/discharge states. The XRD patterns of Li_3PO_4 (JCPDS 87−0039) and metallic Fe (JCPDS 87−0722) are shown for reference for the discharge and recharge products of $LiFePO_4$.

Figure 3a shows the potential profiles of commercial $LiFePO_4$ in the first three cycles between 0.005 and 3.0 V. The long plateau at around 0.6 V corresponds to the decomposition of the $LiFePO_4$ to metallic Fe and Li_3PO_4 in the initial discharge. The capacity for the slope below the plateau is around 300 mAh g^{-1}. High-potential discharge plateaus appear at ~1.7 V in the second and the third cycles. They are attributed to the unreduced (residual) $LiFePO_4$ in the previous discharge. The discharge plateau is much higher than in the initial discharge is supposed to be due to the $LiFePO_4$ particle pulverization and the increase ofz the surface energy of the pulverized particles. These observations are consistent with the report of ref 14. However, we noticed that the charge profile is actually a straight line below 2.0 V and corresponds to a reversible capacity of 260 mAh g^{-1}, although the XRD and HRTEM characterizations have proven that Li_3PO_4 cannot be decomposed until 4.2 V. If the cutoff charge potential is lowered to 1.7 V, then the charge profile becomes almost perfectly straight (Figure 3b). The charge capacity between 0.005 and 1.7 V is 220 mAh g^{-1}, less than ~20 mAh g^{-1} of which comes from the carbon black (CB), the conductive additive in the electrode sheet (the curve at the bottom of Figure 4a shows that the capacity of a Li_3PO_4/CB composite (9:1 by weight) is ~20 mAh g^{-1}). The discharge profiles of the second and subsequent cycles are like arcs, different from the potential profiles of supercapacitors but similar to that of a pseudocapacitor, where electrochemical reactions take place on

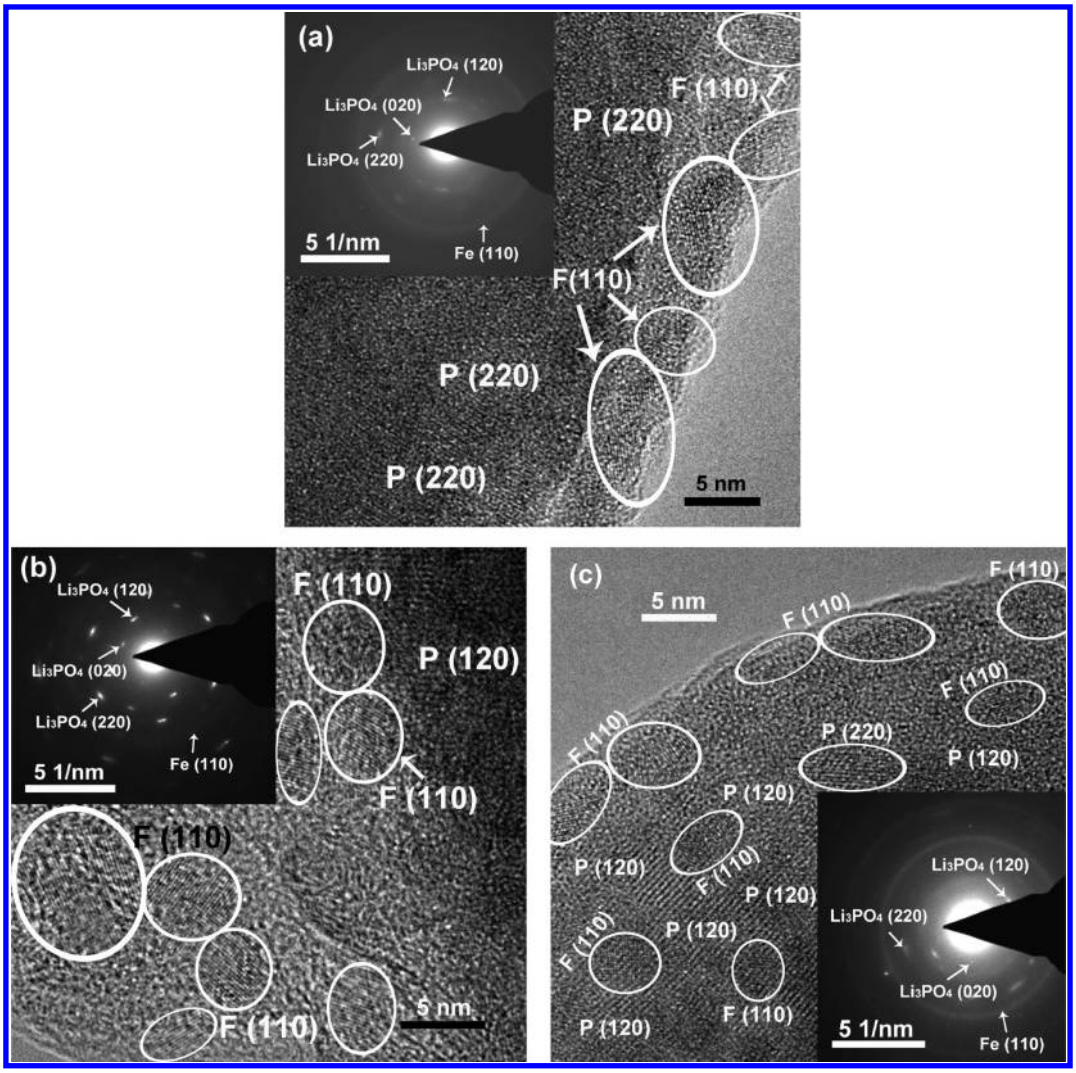

Figure 2. HRTEM images and SAED patterns (insets) of the $LiFePO_4$ at various states: (a) $LiFePO_4$ discharged to 0.005 V, (b) Fe/Li_3PO_4 composite recharged to 1.7 V, and (c) 4.2 V. F is for Fe and P is for Li_3PO_4 in the HRTEM images.

Table 1. Comparison of the *d* Value, Relative Intensity (RI, the RI of the Strongest Line Is Defined As 999), and the Index of the Strongest Diffraction Lines of Li_3PO_4, $LiFePO_4$, and Metallic Fe in the XRD Patterns and the Indexing of the HRTEM and SAED Results

$LiFePO_4$ (83−2092)			Li_3PO_4 (87−0039)			Fe (87−0722)			*d* (±0.03 Å) value by this work		
d (Å)	RI	index	*d* (Å)	RI	index	*d* (Å)	RI	index	HRTEM	SAED	index
						2.0228	**999**	**110**	2.01	2.04	Fe(110)
2.5208	999	311	**2.6418**	**305**	**220**				2.65	2.66	Li_3PO_4(220)
3.4825	832	111/201	**3.9808**	**999**	**120**				3.96	3.98	Li_3PO_4(120)
			5.2430	**267**	**020**				5.22	5.23	Fe(020)
3.0050	781	211/020	3.8375	955	102	1.1679	175	211			
4.2730	761	101	3.5908	529	021	1.4303	115	200			

a [a] The diffraction lines with the nearest spacing values are listed in the same line for comparison; and the bottom two lines are just for a complete overview of the *d* values of the materials.

the electrode surface (new chemicals are produced). Arc-like discharge profiles have been observed in thin film electrodes without carbon black for the interfacial storage.[7] The reason for this is not yet clear. The capacitive behavior of the Fe/Li_3PO_4 nanocomposite is confirmed with cyclic voltammetry (CV) in Figure 3c,d. The CV curve is roughly rectangular without any obvious redox peaks between 0.005 and 1.7 V, characteristic of the electrode materials in a supercapacitor. The higher the

dx.doi.org/10.1021/jp111015j |*J. Phys. Chem. C* 2011, 115, 3803–3808

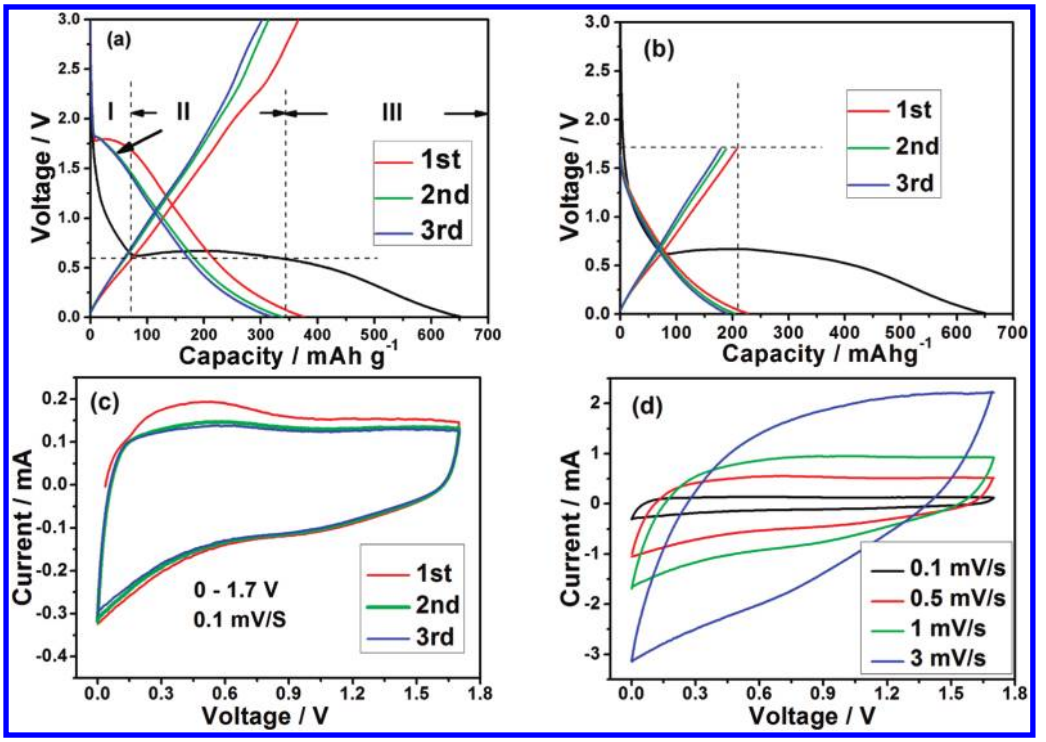

Figure 3. The potential profiles of the commercial $LiFePO_4$ cycled (a) between 0.005 and 3.0 V and (b) between 0.005 and 1.7 V at a current density of 0.10 mA cm^{-2}. Parts (c) and (d) are for the CV traces of the Fe/Li_3PO_4 composite between 0.000 and 1.7 V at 0.05 mV s^{-1}.

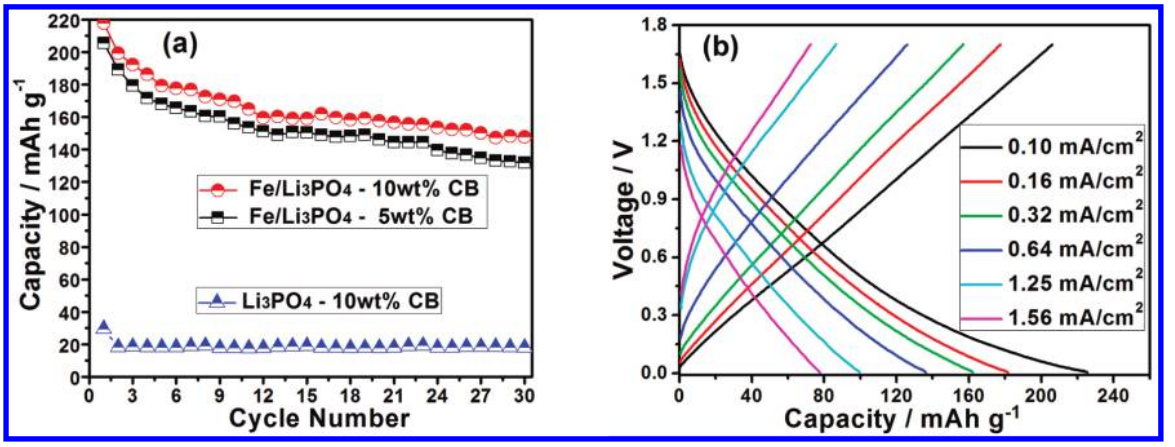

Figure 4. The cycling stability at a current density of 0.10 mA cm^{-2} (a) and the rate performance (b) of the Fe/Li_3PO_4 composite between 0.005 and 1.7 V after the first discharge of the commercial $LiFePO_4$. The curve at the bottom of (a) is for the capacity of a Li_3PO_4/CB composite (9:1 w/w) at 0.1 mA g^{-1} between 0.005 and 3.0 V.

cycling/scanning rate for the nanocomposite, the more the CV profile is like that in a supercapacitor.[15]

The capacity retention of the Fe/Li_3PO_4 composite is pretty good (Figure 4a). Roughly 60% of the initial charge capacity is remained after 30 galvanostatic cycles at 0.10 mA cm^{-2} current density. Figure 4b indicates that the composite has good rate performances. In addition, the specific capacity of the composite decreases from 220 to 80 mAh g^{-1} as the current density increases from 0.1 to 1.56 mA cm^{-2}.

As nanosized iron can have a strong catalytic effect, it might be argued that the obtained capacity is due to the decomposition of the solid electrolyte interphase (SEI) layer formed in the initial discharge. Fourier transformed infrared (FTIR) spectra of commercial Li_3PO_4 and $LiFePO_4$ are compared with that of the in situ obtained Fe/Li_3PO_4 nanocomposites charged to various voltages (Figure 5). It is seen that the FTIR spectrum of the Fe/Li_3PO_4 composite recharged to 1.7 V is very similar to that of the $LiFePO_4$ discharged to 0.005 V between 1200 and 1700 cm^{-1}, meaning that no obvious SEI decomposition occurs below 1.7 V. This indicates that the charge capacity below 1.7 V should not be attributed to the decomposition of the SEI layer.

The FTIR spectrum of the composite charged to 2.0 V, however, is drastically different from that of the composite charged to 1.7 V but slightly similar to that charged to 3.0 V. This means that the decomposition of the organic species such as $ROCO_2Li$ (peaks at 1644, 1451, and 1329 cm^{-1})[16] begins at 2.0

dx.doi.org/10.1021/jp111015j |J. Phys. Chem. C 2011, 115, 3803–3808

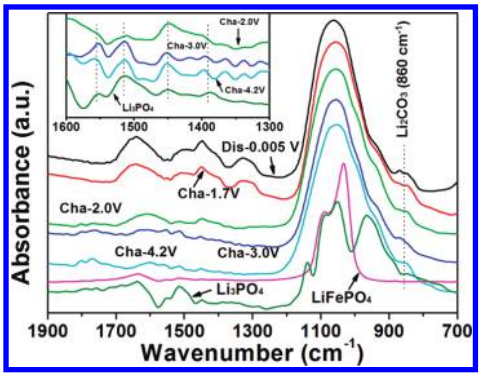

Figure 5. Comparison of the FTIR spectra of the commercial Li_3PO_4, commercial $LiFePO_4$ and commercial $LiFePO_4$ discharged and recharged to various potentials. The inset compares the selected spectra of the commercial Li_3PO_4 and the Fe/Li_3PO_4 nanocomposite recharged to various potentials.

V and almost finishes at 3.0 V. Above 3.0 V, Li_2CO_3 becomes the dominant SEI components on the electrode (the 1506 cm^{-1} band of Li_2CO_3 overlaps with the stronger 1512 cm^{-1} band of Li_3PO_4 in the inset). Usually, the SEI layer is stable up to 3.0 V vs Li^+/Li on graphitic anodes. The decomposition of the SEI layer at a lower potential here is attributed to the catalysis effect of the metallic Fe nanoparticles.

In addition, the spectral details of the characteristic peaks of PO_4^{3-} at ~1060 cm^{-1} become unrecognizable in the discharged and recharged samples. However, the weak peaks of Li_3PO_4 in the discharged $LiFePO_4$ are still recognizable in the Fe/Li_3PO_4 composite charged to 4.2 V (inset in Figure 5), in accordance with the XRD and HRTEM results, that is, both Fe and Li_3PO_4 are stable up to 4.2 V.

Considering that the SEI layer is stable until 1.7 V and the Fe and Li_3PO_4 nanograins are electrochemically inactive below 4.2 V, the lithium storage capacity in the Fe/Li_3PO_4 composites below 1.7 V can neither be attributed to the electrochemical conversion reaction between Li_3PO_4 and metallic Fe nor the electrochemical decomposition of the SEI layer. It is a purely capacitive charge-storage behavior. On the basis of Maier's previous reports, the charges are believed to be stored on the interfaces or the boundaries of the Fe and the Li_3PO_4 nanograins. That is, the lithium ions and electrons are stored, respectively, on the interior surfaces of the Li_3PO_4 and Fe crystallites. In addition, the nanograins of metallic Fe and Li_3PO_4 are randomly dispersed in the sample. As there does not exist a clear interface between the Fe and Li_3PO_4 nanograins (Figure 2), we believe that it is probably more exact to define the lithium storage as on the boundaries of the metallic Fe and Li_3PO_4 grains rather than on their interfaces.

Capacity decay is observed in Figure 4a. Similar capacity fading has been reported in Ti/LiF composite thin film electrodes.[7] The reason for the capacity decay is not explicit at present. The "electrochemical Ostwald ripening" effect[17] might be responsible for the capacity decay in the nanocomposite electrode, that is, the nanocrystallites grow in size with cycling to reduce their surface energies. Therefore, the size of the Fe and Li_3PO_4 nanograins grow and their SSAs decrease with continuous cycling. Loss of electric contact between the electrode material and the current collector might be another reason for this. More research needs to be done to clarify the reason for capacity decay.

CONCLUSIONS

Purely capacitive energy storage has been realized in Fe/Li_3PO_4 nanocomposites obtained by discharging commercial $LiFePO_4$ to 0.005 V vs Li^+/Li. The reversible capacity of the composite reaches 220 mAh g^{-1} between 0.005 and 1.7 V, although both the Fe and Li_3PO_4 nanograins are stable up to 4.2 V and the SEI layer decomposition does not occur until 1.7 V. The electrons and lithium ions are stored on the boundaries of the Fe and Li_3PO_4 nanograins. In addition, the presence of the Fe nanograins lowers the decomposition potential of the organic species in the SEI layer to ~2.0 V. Charge storage on the grain boundaries might be a common feature of metal compounds that can be electrochemically decomposed, reversibly or irreversibly, at some appropriate potentials. These findings help in understanding the origin of the long slope in the potential profiles of transition metal compound anode materials and may open up a new way to enhance the specific capacity and the rate performance of the electrode materials for lithium ion batteries.

AUTHOR INFORMATION

Corresponding Author

*E-mail: zxwang@aphy.iphy.ac.cn(Z.X.W.); lqchen@aphy.iphy.ac.cn (L.Q.C.).

ACKNOWLEDGMENT

This work was financially supported by the National 973 Program of China (2009CB220100) and the WCU (World Class University) program through the Korea Science and Engineering Foundation funded by the Ministry of Education, Science and Technology of Korea (*R*32-2009-000-20074-0).

REFERENCES

(1) (a) Wu, N.-L. *Mater. Chem. Phys.* **2002**, *75*, 6. (b) Simon, P.; Gogotsi, Y. *Nat. Mater.* **2008**, *7*, 845.

(2) Poizot, P.; Laruelle, S.; Grugeon, S.; Dupont, L.; Tarascon, J.-M. *Naure.* **2000**, *407*, 496.

(3) Bruce, P. G.; Scrosati, B.; Tarascon, J.-M. *Angew. Chem., Int. Ed.* **2008**, *47*, 2930.

(4) Jamnik, J.; Maier, J. *Phys. Chem. Chem. Phys.* **2003**, *5*, 5215.

(5) Zhukovskii, Y. F.; Balaya, P.; Kotomin, E. A.; Maier, J. *Phys. Rev. Lett.* **2006**, *96*, 059302.

(6) Zhukovskii, Y. F.; Balaya, P.; Dolle, M.; E. Kotomin, A.; Maier, J. *Phys. Rev. B.* **2007**, *76*, 235414.

(7) Yu, X. Q.; Sun, J. P.; Tang, K.; Li, H.; Huang, X. J.; Dupont, L.; Maier, J. *Phys. Chem. Chem. Phys.* **2009**, *11*, 9497.

(8) Liao, P.; MacDonald, B. L.; Dunlap, R. A.; Dahn, J. R. *Chem. Mater.* **2008**, *20*, 454.

(9) Balaya, P.; Li, H.; Kienle, L.; Maier, J. *Adv. Funct. Mater.* **2003**, *13*, 621.

(10) (a) Poizot, P.; Laruelle, S.; Grugeon, S.; Dupont, L.; Tarascon, J.-M. *J. Electrochem. Soc.* **2002**, *149*, A1212. (b) Silva, D. C. C.; Crosnier, O.; Ouvrard, G.; Greedan, J.; Safa-Sefat, A.; Nazar, L. F. *Electrochem. Solid-State Lett.* **2003**, *6*, A162.

(11) Li, H.; Richter, G.; Maier, J. *Adv. Mater.* **2003**, *15*, 736.

(12) Laruelle, S.; Grugeon, S.; Poizot, P.; Dolle, M.; Dupont, L.; Tarascon, J. -M. *J. Electrochem. Soc.* **2002**, *149*, A627.

(13) Dedryvere, R.; Laruelle, S.; Grugeon, S.; Poizot, P.; Gonbeau, D.; Tarascon, J. -M. *Chem. Mater.* **2004**, *16*, 1056.

(14) Kalaiselvi, N.; Doh, C. H.; Park, C. W.; Moon, S. I.; Yun, M. S. *Electrochem. Commun.* **2004**, *6*, 1110.

(15) (a) Yang, X. Q.; Wu, D. C.; Chen, X. M.; Fu, R. W. *J. Phys. Chem. C* **2010**, *114*, 8581. (b) Kim, B.; Chung, H.; Kim, W. *J. Phys. Chem. C* **2010**, *114*, 15223.

(16) (a) Aurbach, D.; Daroux, M. L.; Faguy, P. W.; Yeager, E. *J. Electrochem. Soc.* **1987**, *134*, 1611. (b) Aurbach, D.; Ein-Eli, Y.; Markovsky, B.; Zaban, A.; Luski, S.; Cameli, Y.; Yamin, H. *J. Electrochem. Soc.* **1995**, *142*, 2882.

(17) Schro1der, A.; Fleig, J.; Gryaznov, D.; Maier, J.; Sitte, W. *J. Phys. Chem. B.* **2006**, *110*, 12274.